Nuclear Inst. and Methods in Physics Research, A 868 (2017) 122–128

Contents lists available at ScienceDirect

Nuclear Inst. and Methods in Physics Research, A

journal homepage: www.elsevier.com/locate/nima

A new response matrix for a ^{6}LiI scintillator BSS system

M.A.S. Lacerda [a,*], R. Méndez-Villafañe [b], A. Lorente [c], S. Ibañez [c], E. Gallego [c], H.R. Vega-Carrillo [d]

[a] Laboratório de Calibração de Dosímetros, Centro de Desenvolvimento da Tecnologia Nuclear, CDTN/CNEN, Av. Presidente Antônio Carlos, 6627, 31270-901, Belo Horizonte, Brazil

[b] Laboratorio de Patrones Neutrónicos, Centro de Investigaciones Energéticas, Medioambientales y Tecnológicas, CIEMAT, Av. Complutense, 22, 28040, Madrid, Spain

[c] Departamento de Ingenieria Energética, Universidad Politécnica de Madrid, UPM, 28006, Madrid, Spain

[d] Unidad Academica de Estudios Nucleares, Universidad Autonoma de Zacatecas, C. Cipres 10, Fracc. La Peñuela, 98068 Zacatecas, Zac, Mexico

ARTICLE INFO

Keywords:
Neutron spectrum
Bonner sphere
Response matrix
Monte Carlo

ABSTRACT

A new response matrix was calculated for a Bonner Sphere Spectrometer (BSS) with a ^{6}LiI(Eu) scintillator, using the Monte Carlo N-Particle radiation transport code MCNPX. Responses were calculated for 6 spheres and the bare detector, for energies varying from 1.059E(−9) MeV to 105.9 MeV, with 20 equal-log(E)-width bins per energy decade, totalizing 221 energy groups. A comparison was done among the responses obtained in this work and other published elsewhere, for the same detector model. The calculated response functions were inserted in the response input file of the MAXED code and used to unfold the total and direct neutron spectra generated by the ^{241}Am-Be source of the Universidad Politécnica de Madrid (UPM). These spectra were compared with those obtained using the same unfolding code with the Mares and Schraube matrix response.

1. Introduction

Neutron spectrometry is important for complete characterization of the radiation field in workplaces. From the neutron fluence spectrum, it is possible to determine direction-independent quantities, such as ambient dose equivalent H*(10). Bonner sphere spectrometer (BSS), also known as Multisphere spectrometer, is normally used for neutron spectrometry studies. BSS have the advantage of an almost isotropic response, covering a wide energy range from thermal to GeV [1–4].

BSS consist of a thermal neutron detector surrounded by a set of moderating polyethylene spheres of varying thickness. When the detector/moderator is uniformly irradiated, there is a response function, defined as the reading per unit fluence, as function of neutron energy. The response function is normally calculated using Monte Carlo (MC) codes and validated with measurements performed in standardized monoenergetic neutron fields [4,5].

From the response functions, a response matrix (R) with "$m \times n$" values are created, where "m" represents the matrix rows or the number of detector/moderating spheres and "n" stands for the total number of energy bins considered. The Response matrix (R) and BSS readings (M), assumed contained in a vector of "n" elements, are used to obtain the spectral information, Φ, also assumed contained in a vector with "n" elements. Then, a set of "m" linear equations can be written as showed in Eq. (1).

$$M = R \cdot \Phi. \tag{1}$$

Neutron spectrum is derived by applying an inverse process, called unfolding procedure, that is a typical few-channel unfolding, since the number of individual measurements, "m", is significantly smaller than the number of energy bins, "n". A number of unfolding procedures, based on different approaches, have been developed to solve this under-determined problem. Linear and non-linear least-squares adjustments, the Bayesian theory, the principle of maximum entropy, Monte Carlo and approaches based on artificial intelligence technology are the methods used for unfolding [6]. Many computerized BSS unfolding codes have been developed using the methods previously described, such as BON94, BUNKI/BUNKIUT, MAXED, FRUIT, BUMS, NSDUAZ and NSDann [7–13].

A good knowledge of the response matrix of the BSS system is fundamental to obtain reliable spectrometric results. There are some published response functions available for BSS with ^{6}LiI detectors

* Corresponding author. Fax: +55 31 30693425.
E-mail addresses: masl@cdtn.br, madslacerda@gmail.com (M.A.S. Lacerda), roberto.mendez@ciemat.es (R. Méndez-Villafañe), alfredo.lorente@upm.es (A. Lorente), sviatoslav.ibanez@upm.es (S. Ibañez), eduardo.gallego@upm.es (E. Gallego), fermineutron@yahoo.com (H.R. Vega-Carrillo).

http://dx.doi.org/10.1016/j.nima.2017.06.057
Received 28 December 2016; Received in revised form 30 June 2017; Accepted 30 June 2017
Available online 8 July 2017
0168-9002/

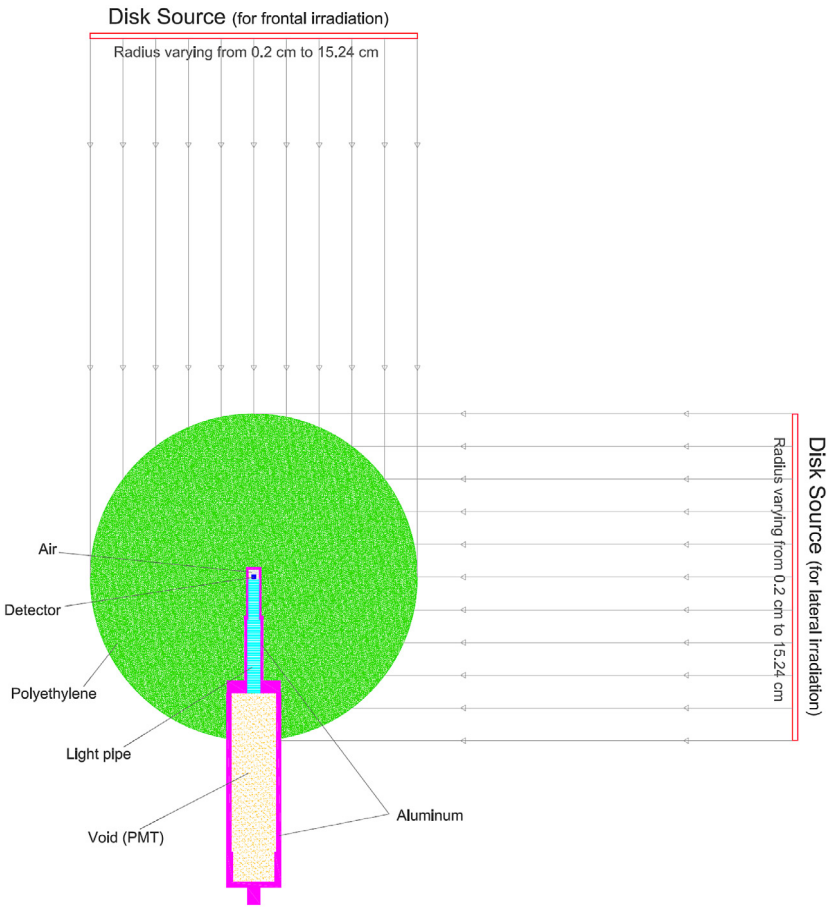

Fig. 1. MCNPX model of the BSS/^{6}LiI(Eu) detector with the 12 inch sphere (BALL 12).

[5,14–17], ^{3}He proportional counters [18–20] and passive detectors [21–23]. An accurate calculation of the response matrix depends, among other things, on the method of solving radiation transport problem, on the accuracy of the cross section data and, on the adequacy of the geometry model [24].

In this work we used the Monte Carlo N-Particle radiation transport code MCNPX [25] to calculate the response functions of a Bonner Sphere Spectrometer (BSS) with a ^{6}LiI(Eu) scintillator. In order to test the response matrix, the total and direct neutron spectra of ^{241}Am-Be neutron source were measured with a BSS with ^{6}LiI(Eu) scintillator at the Universidad Politécnica de Madrid (UPM).

2. Materials and methods

The Monte Carlo N-Particle radiation transport code MCNPX, version 2.7.0, with ENDF/B-VII.0 nuclear data library was used to calculate the response functions of a Bonner Sphere Spectrometer (BSS) with a ^{6}LiI(Eu) scintillator. A realistic model of the cylindrical detector (0.4 cm × 0.4∅ cm) with its metallic cask, the light pipes and the polyethylene spheres was designed. MC calculations were performed for the following sphere diameters, in inches: BALL 2 (2″), BALL 3 (3″), BALL 5 (5″), BALL 8 (8″), BALL 10 (10″) and BALL 12 (12″). Simulations were also performed with the bare detector, without a polyethylene sphere, BALL 0.

Responses were calculated for all spheres and the bare detector for energies varying from 1.059E(−9) to 105.9 MeV, with 20 equal-log(E)-width bins per energy decade, totalizing 221 energy groups. To ensure a uniform irradiation of the spheres, we assumed monoenergetic neutron sources like disks with the same diameters as the spheres. These disks were centered on and perpendicular to the axis of the detector. To evaluate anisotropy influence, we also carried out simulations with the disks positioned laterally. In this case, we used the same 221 energy bins, for the bare detector. For the other spheres, we used the same 101 energy bins used by Mares and Schraube [17,26]. Fig. 1 shows the MCNPX model of the BSS system, with details of the irradiation geometries simulated.

The amount of input files was 2374 ($8 \times 221 + 6 \times 101$). Two ad-hoc Python programs were developed to aid rapid creation of input files for each sphere/energy bin and rapid extraction of the responses from output files.

Atomic composition and physical data were taken from Seltzer and Berger [27]. We used $S(\alpha, \beta)$ cross section tables for polyethylene (density = 0.95 g cm^{-3}) to take into account the chemical binding and crystalline effects on thermal neutron scattering at room temperatures [24]. For the scintillator crystal, we adopted a density of 3.494 g cm^{-3} and the following mass fractions: 4.36E(−2), 1.8E(−1) and 9.546E(−1) for ^{6}Li, ^{7}Li and ^{127}I, respectively.

The environment between the source and the BSS system was treated as void. For each sphere, the response function was defined as the number of reactions (n,p), (n,d), (n,t) and (n,α) occurring within the scintillator, per incident neutron fluence normalized to one starting particle. Response function, R, was calculated using Eq. (2).

$$R = \Phi \cdot a_S \cdot n_{\mathrm{LiI}} \cdot V_{\mathrm{det}} \cdot (\sigma(n,p) + \sigma(n,d) + \sigma(n,t) + \sigma(n,\alpha)) \quad (2)$$

where, Φ is particle fluence, in cm^{-2}, given by the tally 4 in MCNPX, a_S is the area of the neutron source, in cm^2, n_{LiI} is the atomic density of the scintillator in (1E24. cm^{-3}), V_{det} is the detector volume, in cm^3, and $\sigma(n,p)$, $\sigma(n,d)$, $\sigma(n,t)$, and $\sigma(n,\alpha)$ are the cross sections, in barns, for the respective reactions. In MCNPX these reactions are defined as MT = 103, 104, 105, and 107, respectively.

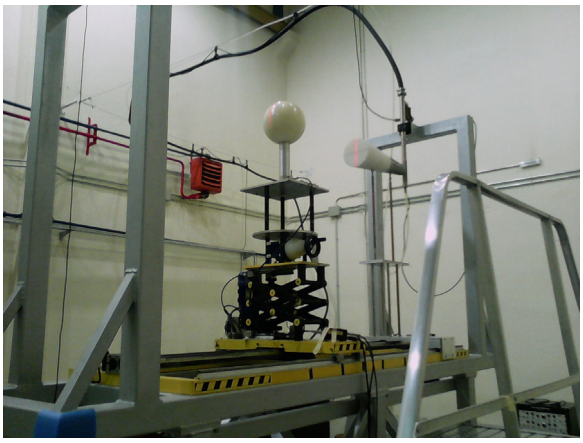

Fig. 2. View of the BSS/^{6}LiI(Eu) on the calibration bench with the 10 inch sphere (BALL 10), and with the shadow cone.

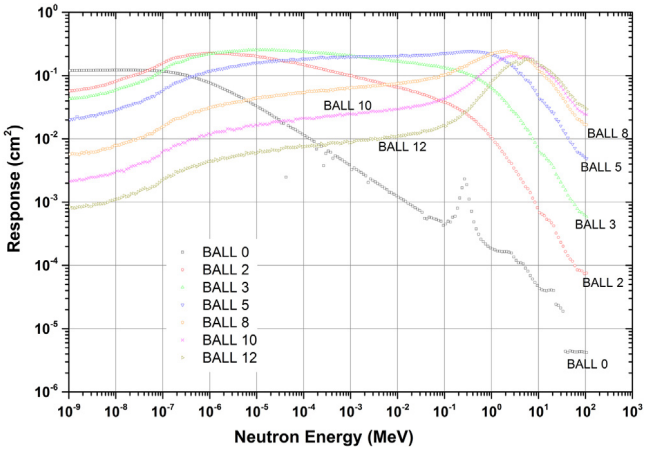

Fig. 3. MCNPX calculated response matrix for the BSS-^{6}LiI.

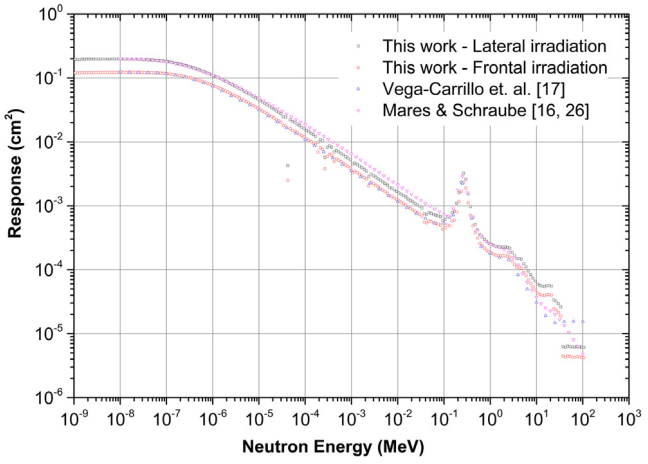

Fig. 4. Comparison of the response function for the bare detector (BALL 0), calculated in this work, and other published data.

The MCNPX was implemented to run under UNIX operating system on the EULER supercomputer, a high performance cluster (HPC) of CIEMAT, composed of 256 blades, 2× Intel Xeon 5450 Quad Core 3.0 GHz processors (2048 cores total). Between 8 and 16 processors were used to parallel processing/simulation of the inputs. The amount of histories used in the calculations was from 1E6 to 8E8 in the aim to obtain uncertainties less than 3%, for each sphere and for each energy bin. The only variance reduction technique used was to assign a double importance to neutrons reaching the ^{6}LiI cell.

A BSS system manufactured by the Ludlum Measurements, like the modeled in this work, was used to measure neutron spectra generated by the ^{241}Am-Be source of the Universidad Politécnica de Madrid (UPM). This source has an activity of 111 ± 10% GBq and a nominal strength of 6.64E(6) s^{-1} on February 5, 1969. The BSS is calibrated at regular basis using the procedure described by Vega-Carrillo et al. [12]. During calibration, the neutron spectra are used to estimate the ambient dose equivalent (H*(10)) and compared with the H*(10) measured with a neutron area monitor Berthold LB6411, calibrated at the Czech Metrology Institute. The overall uncertainties, including the neutron source activity, the anisotropy and the position on the bench was 10.05%. The UPM BSS has also been verified in a comparison between four different BSS [28], three of them calibrated at PTB (Germany) and INFN (Italy).

Measurements were performed at 115 cm from the source, on the calibration bench with and without the shadow cone (SC). Fig. 2 shows a view of the BSS/6LiI(Eu) on the calibration bench with the 10 inch sphere (BALL 10), and with the shadow cone.

BSS was used in combination with a Multichannel analyzer in order to separate the gamma signal from the neutron signal in the scintillator. For each sphere the measuring times were long enough to have 10 000 counts in order to have uncertainties around 1%. Measured counts were normalized to the multichannel live time in order to obtain the count rates that were used to unfold the total (Φ_{tot}) and the direct ($\Phi_{dir} = \Phi_{tot} - \Phi_{SC}$) neutron spectra, where Φ_{SC} is the neutron spectrum measured with the SC. Unfolding was performed with the MAXED computer code, from the UMG 3.3 package [29], with the new calculated response functions.

The initial guess spectra used were those obtained with Monte Carlo calculations, from a previous model of the irradiation facility [12]. To unfold direct spectra (Φ_{dir}) we used the Monte Carlo model replacing the concrete of the walls with the air, to exclude room scattering. The neutron energy spectra were folded with fluence-to-ambient dose equivalent conversion coefficients, in pSv cm^2, from the ICRP 74 [30].

Response functions of Mares and Schraube [17,26] were also inserted in the response input file of the MAXED computer code of the UMG 3.3 package to unfold total and direct spectra generated by the ^{241}Am-Be source of the UPM. Spectra unfolded with the response matrix calculated in this work were compared with those obtained with the Mares and Schraube response matrix.

3. Results and discussions

Fig. 3 presents the MCNPX calculated response matrix for all spheres, 221 energy bins and frontal irradiation geometry. Figs. 4–7 show a comparison of the response function for each sphere, calculated in this work, and data published by Vega-Carrillo et al. [17] and Mares and Schraube [16], for the same model of BSS system. Additional data provided by Mares and Schraube [26], with the inclusion of more energy bins, were included in these graphs. Results for the two irradiation geometries (frontal and lateral) are included in the comparisons. The ratios between the responses obtained in this work and Mares and Schraube [16,26], for all spheres, are presented in Fig. 8. The ratios between the responses obtained with frontal and lateral irradiation geometries, for all energy range, are presented in Figs. 9 and 10.

Fig. 3 shows the response functions for all spheres presented an agreement in shape with other available in literature [16,17,31]. Figs. 4–7 show a comparison of our data and other published elsewhere, for the same detector model. For the frontal irradiation setup, BALL 0 responses agreed well with Vega-Carrillo et al. [17] and did not agree well with Mares and Schraube [16,26]. The bare detector (BALL 0) presented a shape close to the shape of the ^{6}Li$(n,t)^{4}$He cross section. For

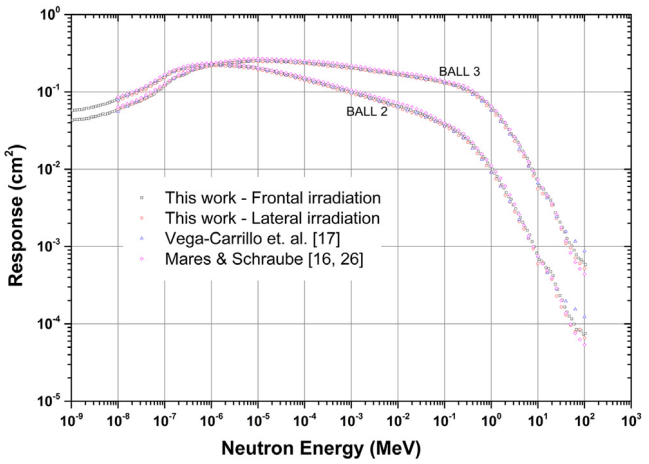

Fig. 5. Comparison of the response function for detector with the 2 inch and 3 inch sphere (BALL 2 and BALL 3), calculated in this work, and other published data.

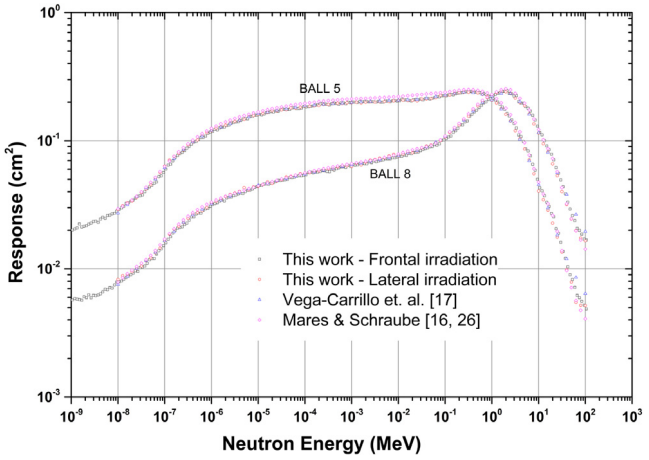

Fig. 6. Comparison of the response function for detector with the 5 inch and 8 inch sphere (BALL 5 and BALL 8), calculated in this work, and other published data.

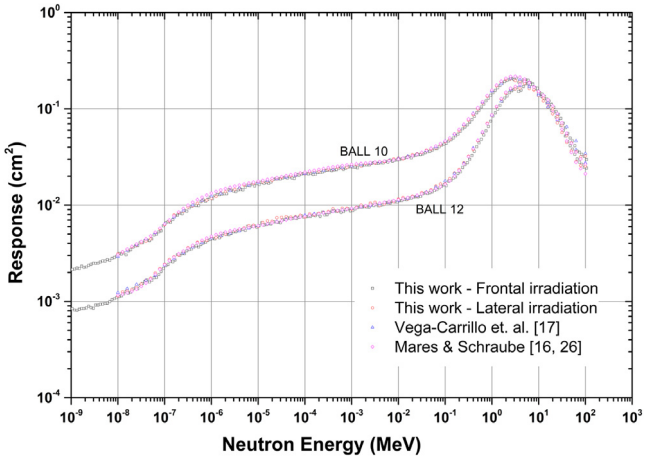

Fig. 7. Comparison of the response function for detector with the 10 inch and 12 inch sphere (BALL 10 and BALL 12), calculated in this work, and other published data.

energies above 20 MeV, an anomalous behavior is noticed for the BALL 0. We can observe a rapid decreasing followed by an almost constant response. These observations can be attributed to the differences in cross-section libraries. As the ENDF/B-VII.0 nuclear data library does

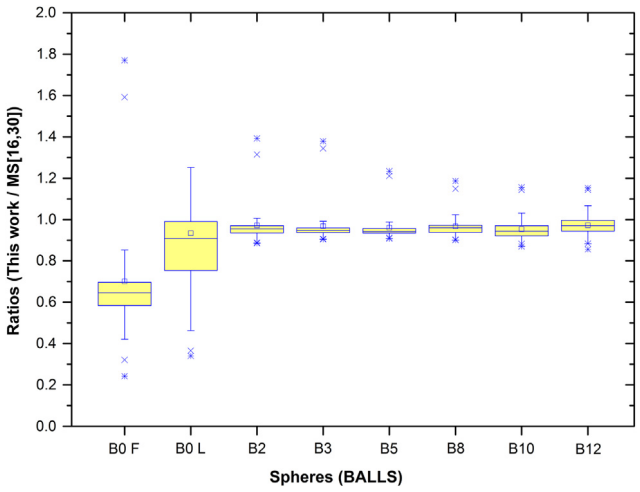

Fig. 8. Variation of the ratios between the responses obtained in this work and Mares and Schraube [16,26], for all spheres.

not have available data for energies higher than 20 MeV, MCNPX uses a constant cross section equal to the value at 20 MeV. This adopted value is supposed to be much higher than the real cross section values for energies between 20 and 105.9 MeV.

Fig. 8 shows the variation of the ratios between the responses obtained in this work and Mares and Schraube [16,26], for all spheres. For the BALL 0, these ratios were, in average, 0.70. The minimum, maximum, median, 25 and 75 percentile ratios were, respectively, 0.24, 1.77, 0.65, 0.58 and 0.70. That is, 75% of the ratios were less than or equal to 0.70. These ratios are higher than 1.0, only for the 9 bins with energies varying from 3.981 to 31.62 MeV. For energies lower than 10 MeV, the ratios are minor than or equal to 1.22. The agreement is improved, when we consider the lateral irradiation geometry. In this case, the ratios for the BALL 0 were, in average, 0.93, and varied from 0.34 to 2.35. The median, 25 and 75 percentile ratios were, respectively, 0.91, 0.75 and 0.99. For neutrons with energies lower than 10.00 MeV, 66% of the ratios varied from 0.76 to 1.16. The worst ratios, in this case, were found for the three bins with energies varying from 10.00 to 19.95 MeV, respectively, 1.83, 2.23 and 2.35. For the other spheres, the agreement with published responses [16,17,26] were better than 14%. The third quartile of the ratios for these spheres were lower than 1.00. Ratios higher than 1.00 are usually found only for the bins with energies higher than about 5.0 MeV. The differences in responses calculated in this work with Mares and Schraube responses [16,26], can be attributed to the differences in cross-section libraries, mass densities and ^{6}Li enrichment.

Figs. 9 and 10 show the ratios of the responses obtained with frontal and lateral irradiation geometries, for all energy range. The frontal geometry of irradiation underestimates responses for BALL 0. Already, for BALLS 2 and 3, the opposite is observed for almost all energy interval. For BALLS 8, 10 and 12, the ratios are between 0.88 and 1.16. Not considering the BALL 0, the worst ratios were found for BALLS 2 and 3 for energies higher than 3.981 MeV.

The reaction (n,t) contributes with more than 99.8% on response functions for all detector/spheres. Exceptions are the spheres 0, 2 and 3, for energies higher than 3.76 MeV. Fig. 11 shows, for these spheres and range of energies, the contribution of each reaction on responses. We can observe that reaction (n,p) contributes significantly on response functions for the BALLS 0 and 2 and less than 1% for the BALL 3. For the BALL 0, (n,α) reaction can contribute with more than 5% on response functions for energies close to 20 MeV. For the BALL 2, (n,α) contribution is less than 0.5% and for the BALL 3, less than 0.06%.

Figs. 12 and 13 show, respectively, the total (Φ_{tot}) and direct (Φ_{dir}) neutron lethargy spectra measured with the UPM BSS-^{6}LiI system. Data

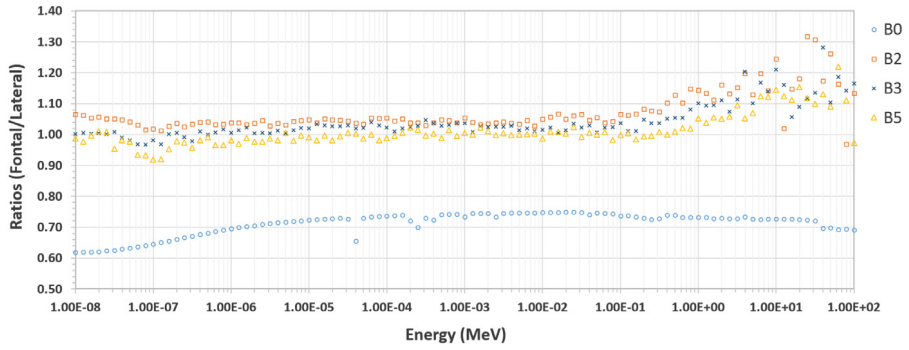

Fig. 9. Ratios of the responses obtained with frontal and lateral irradiation geometries, for all energy range and BALLS 0, 2, 3 and 5.

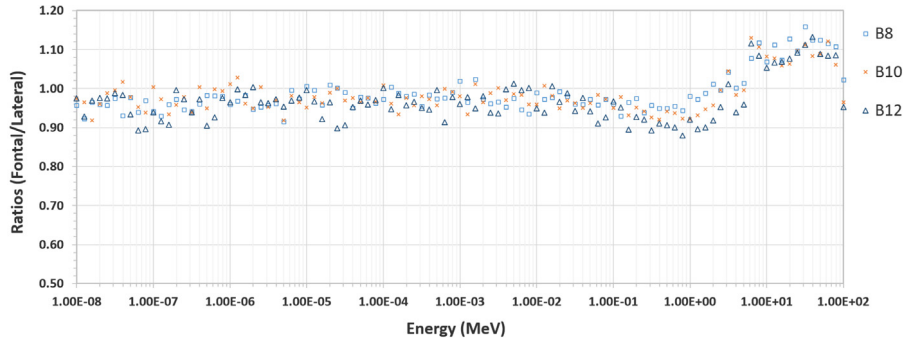

Fig. 10. Ratios of the responses obtained with frontal and lateral irradiation geometries, for all energy range and BALLS 8, 10 and 12.

were unfolded with the MAXED computer code, with the new response matrix, calculated in this work, and Mares and Schraube matrix [16,26]. For the response matrix calculated in this work, we considered two cases: (a) all responses calculated considering the frontal irradiation geometry and; (b) only the Ball 0 responses considering the lateral irradiation geometry. The direct spectrum was unfolded without BALL 0, once we did not performed measurements with the bare detector and the shadow cone.

Table 1 shows a comparison of the quantities: total fluence and fluence components (thermal, epithermal and fast), ambient dose equivalent (H*(10)) and average energy, for the total (Φ_{tot}) and direct (Φ_{dir}) spectra. For the MAXED code, the uncertainties in the total fluence and H*(10) are those provided by the software IQU_FC33, from the UMG 3.3 package. IQU_FC33 considers variations in the measured data and in the default spectrum and uses standard methods to do sensitivity analysis and uncertainty propagation [29]. We did not take into account the uncertainties in the calibration of the spectrometer and in the response matrix. Energy ranges considered for the fluence components are: below 0.5 eV for thermal neutrons, between 0.5 eV and 0.1 MeV for epithermal, and above 0.1 MeV for fast neutrons.

Total and direct spectra unfolded with the matrix responses calculated in this work (only B0 Lateral) show a relatively good agreement with those obtained with the Mares and Schraube matrix [16,26]. Total fluence, H*(10) and the average energy, for both spectra, agreed within 4.8% and 3.8%, respectively. There were observed, also, a good agreement in the fluence components.

4. Conclusions

A new response matrix was calculated for a Bonner Sphere Spectrometer (BSS) with a ^{6}LiI(Eu) scintillator, using the Monte Carlo N-Particle radiation transport code MCNPX. Responses were calculated for 6 spheres and the bare detector, for energies varying from 1.059E(−9) to 105.9 MeV, with 20 equal-log(E)-width bins per energy decade, totalizing 221 energy groups. Different irradiation geometries (frontal and lateral) were simulated, to evaluate the anisotropy influence. A comparison was done among the responses obtained in this work and other published elsewhere [16,17,31], for the same detector model.

The response functions for all spheres presented an agreement in shape with other available in literature [16,17,31]. For the frontal irradiation setup, responses for all spheres agreed well with those published by Vega-Carrillo et al. [17], for energies lower than 20 MeV. However, there were not observed a good agreement of the BALL 0 responses with Mares and Schraube [16,26]. The agreement was improved, when was considered the lateral irradiation geometry. The differences in responses calculated in this work with Mares and Schraube responses [16,26], can be attributed to the differences in cross-section libraries, mass densities and ^{6}Li enrichment.

The calculated response functions were inserted in the response input file of the MAXED code and used to unfold the total and direct neutron spectra generated by the ^{241}Am-Be source of the Universidad Politécnica de Madrid (UPM). These spectra were compared with those obtained using the same unfolding code with the Mares and Schraube matrix [16,26]. Total and direct spectra showed a relatively good agreement with those obtained with the Mares and Schraube matrix [16,26], when was used the B0 response, obtained considering the lateral irradiation geometry. Total fluence and fluence components (thermal, epithermal and fast), ambient dose equivalent (H*(10)) and average energy also showed a good agreement.

The response matrix calculated in this work can be used together with the MAXED code to generate neutron spectra with a good energy resolution up to about 11 MeV. Some additional tests are being done to validate this response matrix and improve the results for higher energies.

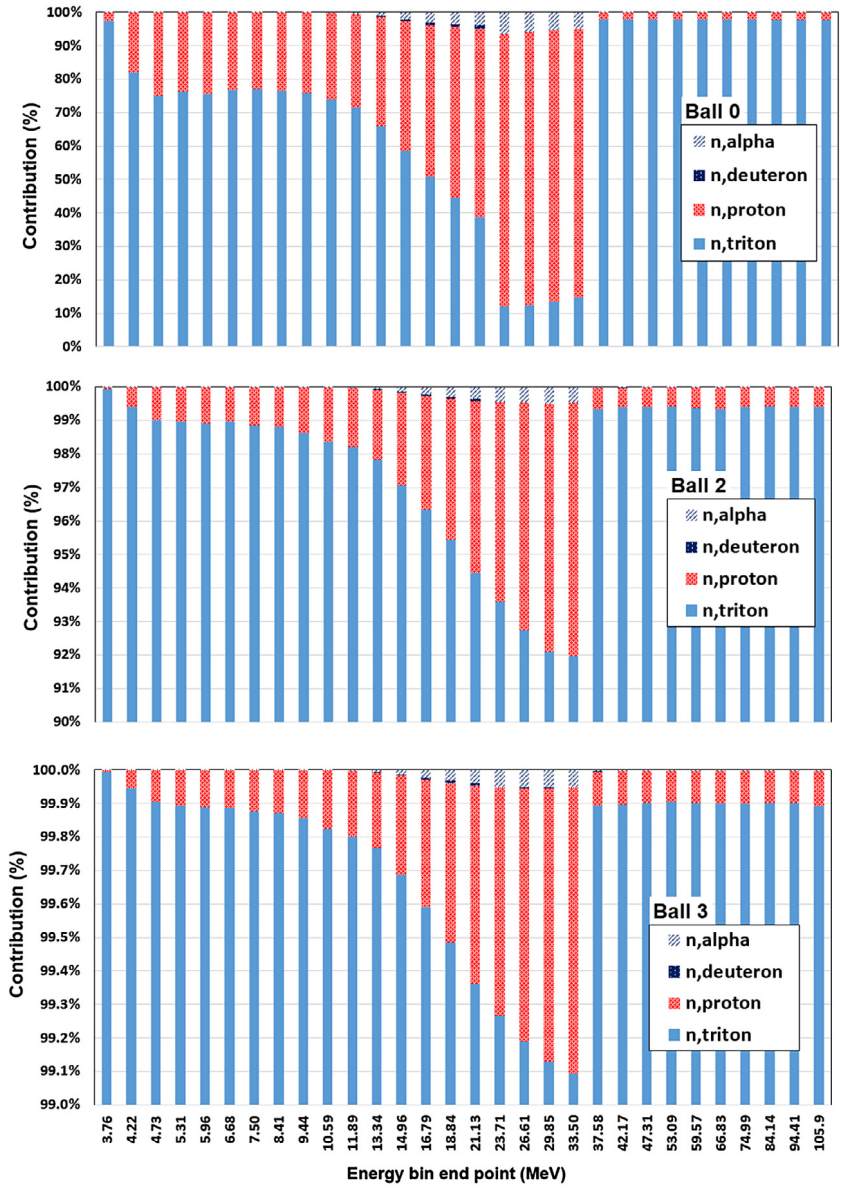

Fig. 11. Contribution of each reaction on response function of the bare detector (BALL 0), 2 inch sphere (BALL 2) and 3 inch sphere (BALL 3).

Table 1
Comparison of the quantities: total fluence and fluence components (thermal, epithermal and fast), ambient dose equivalent rate (H*(10)) and average energy for the total (Φ_{tot}) and direct (Φ_{dir}) spectra.

Mares and Schraube [16,26]	Total (Φ_{tot})		Direct (Φ_{dir})	
	Value	unc (%)	Value	unc (%)
Total fluence rate (cm^{-2} s^{-1})	4.97E+01	5.50E−01	3.89E+01	6.63E−01
$\Phi_{thermal}$	4.22E−02		7.87E−04	
$\Phi_{epithermal}$	8.66E−02		3.26E−02	
Φ_{fast}	8.71E−01		9.67E−01	
H*(10) (μSv/h)	6.18E+01	1.01E+00	5.41E+01	7.40E−01
Average energy (MeV)	3.19E+00		3.79E+00	
This work—only B0 Lateral				
Total fluence rate (cm^{-2} s^{-1})	5.20E+01	4.35E−01	4.07E+01	6.55E−01
$\Phi_{thermal}$	4.05E−02		1.01E−03	
$\Phi_{epithermal}$	8.69E−02		3.10E−02	
Φ_{fast}	8.73E−01		9.68E−01	
H*(10) (μSv/h)	6.40E+01	6.86E−01	5.61E01	7.35E−01
Average energy (MeV)	3.19E+00		3.87E+00	

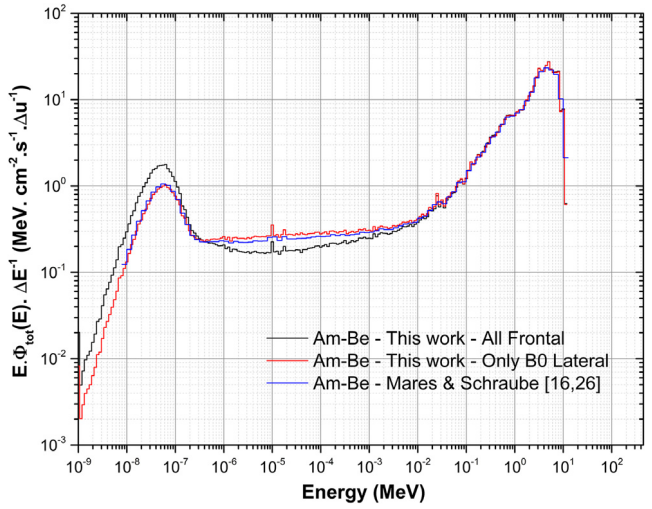

Fig. 12. Comparison of the Total Neutron Lethargy spectra (Φ_{dir}) measured with the BSS-^{6}LiI.

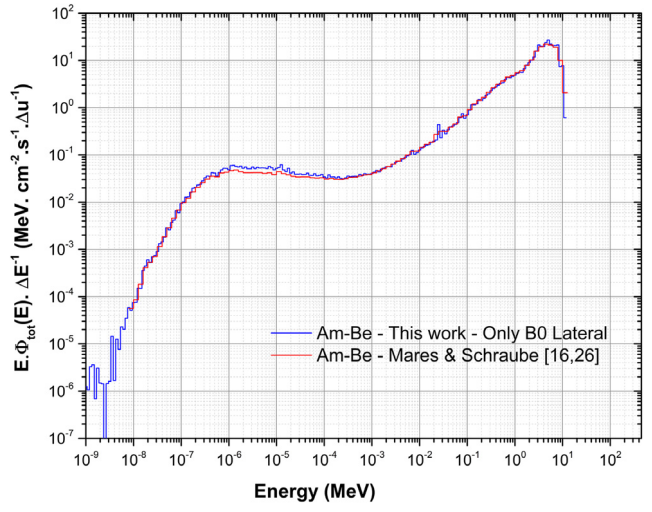

Fig. 13. Comparison of the Direct Neutron Lethargy spectra (Φ_{dir}) measured with the BSS-^{6}LiI.

Acknowledgments

M.A.S. Lacerda is grateful to CNPq (Brazilian National Council for Scientific and Technological Development) for a postdoctoral fellowship (Proc. 233341/2014-5). M.A.S. Lacerda is also grateful to financial support provided by CNPq (MCTI/CNPq/Universal Proc. 449199/2014-2) and FAPEMIG (Research Support Foundation of Minas Gerais State, Brazil) (PPM-00208-15).

References

[1] R.L. Bramblett, R.I. Ewing, T.W. Bonner, A new type of neutron spectrometer, Nucl. Instrum. Methods 9 (1960) 1–12.
[2] M. Awschalow, R.S. Sanna, Applications of Bonner detectors in neutron field dosimetry, Radiat. Prot. Dosim. 10 (1985) 89–101.
[3] D.J. Thomas, A.V. Alevra, Bonner sphere spectrometers–a critical review, Nucl. Instrum. Methods Phys. Res. A 476 (2002) 12–20.
[4] J.C. McDonald, B.R.L. Siebert, W.G. Alberts, Neutron spectrometry for radiation protection purposes, Nucl. Instrum. Methods Phys. Res. A 476 (2002) 347–352.
[5] H. Mazrou, Z. Idiri, T. Sidahmed, M. Allab, MCNP5 evaluation of a response matrix of a Bonner Sphere Spectrometer with a high efficiency ^{6}LiI(Eu) detector from 0.01 eV to 20 MeV neutrons, J. Radioanal. Nucl. Chem. 284 (2010) 253–263.
[6] M. Matzke, Propagation of uncertainties in unfolding procedures, Nucl. Instrum. Methods Phys. Res. A 476 (2002) 230–241.
[7] K.A. Lowry, T.L. Johnson, Modifications to recursion unfolding algorithms to and more appropriate neutron spectra, Health Phys. 47 (1984) 587–593.
[8] J. Sweezy, N. Hertel, K. Veinot, Bonner sphere unfolding made simple: an HTML based multisphere neutron spectrometer unfolding package, Nucl. Instrum. Methods Phys. Res. A 476 (2002) 263–269.
[9] M. Reginatto, P. Goldhagen, S. Neumann, Spectrum unfolding, sensitivity analysis and propagation of uncertainties with the maximum entropy deconvolution code MAXED, Nucl. Instrum. Methods Phys. Res. A 476 (2002) 242–246.
[10] R. Bedogni, C. Domingo, A. Esposito, F. Fernandez, FRUIT: an operational tool for multisphere neutron spectrometry in workplaces, Nucl. Instrum. Methods Phys. Res. A 580 (2007) 1301–1309.
[11] A.V. Sannikov, BON94 code for neutron spectra unfolding from Bonner spectrometer data, CERN internal Report CERN/TIS-RP/IR/94–16, 1994.
[12] H.R. Vega-Carrillo, E. Gallego, A. Lorente, I.P. Rubio, R. Méndez, Neutron features at the UPM neutronics hall, Appl. Radiat. Isot. 70 (2012) 1603–1607.
[13] M.R. Martinez-Blanco, J.M. Ortiz-Rodriguez, H.R. Vega-Carrillo, NSDann, a LabVIEW tool for neutron spectrometry and dosimetry based on the RDANN methodology. in: Procc. 9th of the Electronics, Robotics and Automotive Mechanics Conference, CERMA'09, 2009, 131–136.
[14] R.S. Sanna, Thirty-One Group Response Matrices for the Multisphere Neutron Spectrometer over the energy range thermal to 400 MeV, USAEC, Report HASL-267 1973.
[15] N.E. Hertel, J.W. Davidson, The response of Bonner spheres to neutrons from termal energies to 17 3 MeV., Nucl. Instrum. Methods Phys. Res. A 238 (1985) 509–516.
[16] V. Mares, H. Schraube, Evaluation of the response matrix of a bonner sphere spectrometer with lii detector from thermal energy to 100 MeV, Nucl. Instrum. Methods Phys. Res. A 337 (1994) 461–473.
[17] H.R. Vega-Carrillo, I. Donaire, E. Gallego, E. Manzanares-Acuña, A. Lorente, M.P. Iñiguez, A. Martin-Martin, J.L. Gutierrez-Villanueva, Calculation of response matrix of a BSS with ^{6}LiI scintillator, Rev. Mexicana Fís. 54 (2008) 57–62.
[18] V. Mares, G. Schraube, H. Schraube, Calculated neutron response of a Bonner Sphere Spectrometer with ^{3}He counter, Nucl. Instrum. Methods Phys. Res. A 307 (1991) 398–412.
[19] A. Aroua, M. Grecscu, M. Lanfranchi, P. Lerch, S. Prête, J.F. Valley, Evaluation and test of the response matrix of a multisphere neutron spectrometer in a wide energy range Part II: Simulation, Nucl. Instrum. Methods Phys. Res. A 321 (1992) 305–311.
[20] B. Wiegel, A.V. Alevra, NEMUS-The PTB neutron multisphere spectrometer: Bonner spheres and more, Nucl. Instrum. Methods Phys. Res. A 476 (2002) 36–41.
[21] R. Bedogni, A. Esposito, A. Gentile, M. Angelone, G. Gualdrini, Determination and validation of a response matrix for a passive Bonner Sphere Spectrometer based on gold foils, Radiat. Meas. 43 (2008) 1104–1107.
[22] S. Garny, V. Mares, W. Rühm, Response functions of a Bonner sphere spectrometer calculated with GEANT4, Nucl. Instrum. Methods Phys. Res. A 604 (2009) 612–617.
[23] H.R. Vega-Carrillo, B.W. Wehring, K.G. Veinot, N.E. Hertel, Response matrix for a multisphere spectrometer using ^{6}LiF thermoluminescence dosemeter, Radiat. Prot. Dosim. 81 (1999) 133–140.
[24] B. Wiegel, A.V. Alevra, B.R.L. Siebert, Calculations of the response functions of Bonner spheres with a spherical ^{3}He proportional conter using a realistic detector model, Physikalisch-Technische Bundesanstalt, Report PTB-N-21, 1994.
[25] D.B. Pelowitz, MCNPX User's Manual, Version 2.7.0, Los Alamos National Laboratory, Report LA-CP-11-00438, 2011.
[26] V. Mares, H. Schraube, (Unpublished) results.
[27] S.M. Seltzer, M.J. Berger, Evaluation of the collision stopping power of elements and compounds for electrons and positrons, Int. J. Appl. Radiat. Isot. 33 (1982) 1189–1218.
[28] E. Gallego, K. Amgarou, R. Bedogni, C. Domingo, A. Esposito, A. Lorente, R. Méndez, H.R. Vega-Carrillo, Characterization of a 241AmBe neutron irradiation facility by different spectrometric techniques. in: Proc. 13th International Congress of the International Radiation Protection Association (IRPA-13). Glasgow, 13–18 May, 2012. Available at http://oa.upm.es/19584/.
[29] M. Reginatto, B. Wiegel, A. Zimbal, F. Langner, The 'few-channel' unfolding programs in the UMG package: MXD_FC31 and IQU_FC31, and GRV_FC31, version 3.1, Physikalisch-Technische Bundesanstalt (PTB), 2004.
[30] International Commission on Radiological Protection, Conversion coefficients for use in radiological protection against external radiation, ICRP Publication 74, Ann. ICRP 26 (3–4), 1996.
[31] A.W. Decker, S.R. McHale, M.P. Shannon, J.A. Clinton, J.W. McClory, Novel Bonner sphere spectrometer response functions using MCNP6, IEEE Trans. Nucl. Sci. 62 (2015) 1–6.